Proton decay testing low energy supersymmetry with precision gauge unification

Stefan Pokorski,[1,2] Krzysztof Rolbiecki,[1] and Kazuki Sakurai[1]

[1]*Institute of Theoretical Physics, Faculty of Physics, University of Warsaw,*
Ludwika Pasteura 5, PL–02–093 Warsaw, Poland
[2]*Theoretical Physics Department, CERN, CH-1211 Geneva 23, Switzerland*

We show that gauge coupling unification in supersymmetry (SUSY) models can make a nontrivial interconnection between collider and proton decay experiments. Under the assumption of precise gauge coupling unification in the Minimal Supersymmeric Standard Model, with negligible grand unified theories threshold corrections, the low energy SUSY spectrum and the unification scale are intertwined, and the lower bound on the proton lifetime can be translated into *upper* bounds on SUSY masses. We find that the current limit on $\tau(P \to \pi^0 e^+)$ already excludes gluinos *heavier* than ~ 70 (120 and 200) TeV if their mass ratio to winos, $R \equiv M_3/M_2$, is ~ 1 (3 and 7), respectively. Next generation nucleon decay experiments are expected to bring these upper bounds down to ~ 5 (10 and 15) TeV for $R \sim 1$ (3 and 7).

Proton decay would be the key evidence for grand unified theories (GUTs) [1]. Among possible decay channels, a special role is played by the $p \to \pi^0 e^+$ mode for which the dominant contribution may come from the $D = 6$ operators depending almost exclusively on the X, Y boson mass and the unified gauge coupling. Unification of the gauge couplings in the minimal supersymmeric Standard Model (MSSM) as a link between the supersymmetric spectrum and the GUT spectrum and a window to the GUT physics has been studied intensively. Most such works have focused on constraining the GUT spectrum making simple assumptions on the low energy supersymmetry (SUSY) spectrum. In this study, we take the opposite approach, very similar to the one proposed in the early Ref. [2] with similar motivation.

Following several studies [3,4], we assume that the unification of the gauge couplings is precise within the MSSM without threshold corrections of GUT scale particles. In fact, such a situation can be realized in a class of extra dimensional GUT models, proposed as a solution to the doublet-triplet splitting problem. In such a scenario, the relevant superheavy particles are in general mass degenerate around the compactification scale, leading to small threshold corrections. In particular, in a 6-D orbifold GUT model that breaks the GUT symmetry nonlocal by Wilson lines, the threshold correction exactly vanishes when the size of two extra dimensions are the same [5,6].[1]

On the other hand, the GUT threshold corrections in conventional models depend on the mass ratios between superheavy particles forming incomplete multiplets (such as the colored Higgs and the X, Y bosons in the minimal SU(5)). If those superheavy particles have hierarchical mass spectra, the threshold corrections can become large enough to spoil "*the success of gauge coupling unification in the MSSM*" [5,8]. We stress again that all conclusions derived in this paper are subject to the assumption of the precision gauge coupling unification within the MSSM.

Under the assumption of precise gauge coupling unification (GCU), we show that the low energy SUSY spectrum and the unification scale are intertwined, and the lower bound on the proton lifetime $\tau_{p \to \pi^0 e^+}$ can be translated into *upper* bounds on SUSY masses.[2] This leads to an interesting interconnection between the proton decay experiments and the collider searches, particularly in view of the future progress on both fronts, in cornering supersymmetric spectrum from above and from below.

In general, the $p \to K^+ \nu$ mode, induced by the $D = 5$ operators generated by the colored Higgs exchange

---

[1]Small but not necessarily vanishing threshold corrections are expected in extra dimensional orbifold GUT models with boundary condition GUT breaking [7].

[2]Unlike other upper bounds on SUSY masses based on the arguments of the Higgs boson mass [9] or the neutralino relic abundance [10], these bounds depend neither on the ratio of the Higgs vacuum expectation values, $\tan\beta \equiv v_u/v_d$, nor the assumption of R-parity conservation and the thermal history of the universe.

diagrams, also gives a strong constraint on the colored Higgs mass and low energy SUSY spectrum as well as the structure of the Higgs sector in the GUT models [11]. However, this mode is highly model-dependent, and several mechanisms have been known to suppress it independently of the GCU [12].[3] We therefore do not consider this mode in this paper for simplicity. In any case, the constraints derived from the $p \to \pi^0 e^+$ mode can be applied independently from the $D = 5$ proton decay constraints.

We use the two-loop renormalization group equations (RGEs) for the running of the gauge couplings, which we solve numerically. The solution can be written as [13]

$$\frac{2\pi}{\alpha_i(Q)} = \frac{2\pi}{\alpha_i(m_Z)} - b_i \ln\left(\frac{Q}{m_Z}\right) + s_i + \gamma_i + \Delta_i, \quad (1)$$

where $\alpha_1 \equiv \frac{5}{3}\alpha_Y$, $i = 1, 2, 3$ represents the gauge group, $b_i = (\frac{33}{5}, 1, -3)$ are the one-loop β-function coefficients for the MSSM and

$$s_i \equiv \sum_\eta b_i^\eta \ln\left(\frac{m_\eta}{m_Z}\right) \quad (2)$$

represent the threshold corrections of low energy SUSY particles. The variables m_η and b_i^η denote the mass and the contribution to b_i from the superpartner η. The $\gamma_i \equiv -\frac{1}{2}\sum_j \frac{b_{ij}}{b_j} \ln(\frac{\alpha_j(Q)}{\alpha_j(m_Z)})$ accounts for the two-loop contribution with b_{ij} being the two-loop β-function coefficients.[4] The Δ_i represents the effect of the top Yukawa coupling and the conversion factor between $\overline{\text{MS}}$ and $\overline{\text{DR}}$ schemes.[5]

In the special case where all SUSY particles are mass degenerate at M_s, the threshold correction can be written as $s_i = \delta_i \ln(M_s/m_Z)$ with $\delta_i \equiv (b_i - b_i^{\text{SM}})$, where $b_i^{\text{SM}} = (\frac{41}{10}, -\frac{19}{6}, -7)$ are the one-loop β-function coefficients for the Standard Model (SM). In this case, precision gauge unification $\alpha_1(Q) = \alpha_2(Q) = \alpha_3(Q) \equiv \alpha_G^*$ is achieved by the particular values, $M_s = M_s^*$, $Q = M_G^{\text{deg}*}$, satisfying

$$\frac{2\pi}{\alpha_G^*} = \frac{2\pi}{\alpha_i(m_Z)} - b_i \ln\left(\frac{M_G^{\text{deg}*}}{m_Z}\right) + \delta_i \ln\left(\frac{M_s^*}{m_Z}\right) + \gamma_i + \Delta_i \quad (3)$$

for all i. It should be borne in mind that the quantities M_s^*, $M_G^{\text{deg}*}$ and α_G^* are not variables but constants defined as the solution to the above three simultaneous equations.

Coming back to the general case, let us decompose the vector s_i into three independent vectors as [4]

---

[3]The $D = 5$ proton decays are suppressed also in the class of models discussed in [6,7].

[4]At the unification scale (M_G), it can be approximated as $\gamma_i = -\frac{1}{2}\sum_j \frac{b_{ij}}{b_j} \ln(1 + \frac{b_j \alpha_G}{2\pi} \ln \frac{M_G}{m_Z})$. One can solve γ_i iteratively by updating M_G and α_G.

[5]For the treatment of Δ_i, see for example [14].

$$s_i = \delta_i \ln\left(\frac{T}{m_Z}\right) + b_i \ln\Omega + C. \quad (4)$$

The solution to this set of equations is given by

$$\ln\left(\frac{T}{m_Z}\right) = \frac{v_i s_i}{D} \quad (5)$$

$$\ln\Omega = \frac{u_i s_i}{D} \quad (6)$$

$$C = \frac{\epsilon_{ijk}\delta_j b_i s_k}{D} \quad (7)$$

where summation is understood for the repeated indices and ϵ_{ijk} is the antisymmetric tensor and

$$v = \begin{pmatrix} b_2 - b_3 \\ -b_1 + b_3 \\ b_1 - b_2 \end{pmatrix}, \qquad u = \begin{pmatrix} -\delta_2 + \delta_3 \\ \delta_1 - \delta_3 \\ -\delta_1 + \delta_2 \end{pmatrix},$$

$$D = b_2\delta_1 - b_3\delta_1 - b_1\delta_2 + b_3\delta_2 + b_1\delta_3 - b_2\delta_3. \quad (8)$$

Plugging the concrete values of b_i, δ_i and b_i^η into these expressions, one gets

$$T = [M_3^{-28} M_2^{32} (\mu^4 m_A)^3 X_T]^{\frac{1}{19}}, \quad (9)$$

$$\Omega = [M_3^{-100} M_2^{60} (\mu^4 m_A)^8 X_\Omega]^{\frac{1}{288}}, \quad (10)$$

$$C = \frac{125}{19}\ln M_3 - \frac{113}{19}\ln M_2 - \frac{40}{19}\ln\mu - \frac{10}{19}\ln m_A$$
$$+ \sum_{i=1\ldots3}\left[\frac{79}{114}\ln m_{\tilde{d}_{Ri}} - \frac{10}{19}\ln m_{\tilde{l}_i} - \frac{121}{114}\ln m_{\tilde{q}_i}\right.$$
$$\left. + \frac{257}{228}\ln m_{\tilde{u}_{Ri}} + \frac{33}{76}\ln m_{\tilde{e}_{Ri}}\right], \quad (11)$$

with

$$X_T \equiv \prod_{i=1\ldots3}\left(\frac{m_{\tilde{l}_i}^3}{m_{\tilde{d}_{Ri}}^3}\right)\left(\frac{m_{\tilde{q}_i}^7}{m_{\tilde{e}_{Ri}}^2 m_{\tilde{u}_{Ri}}^5}\right), \quad (12)$$

$$X_\Omega \equiv \prod_{i=1\ldots3}\left(\frac{m_{\tilde{l}_i}^8}{m_{\tilde{d}_{Ri}}^8}\right)\left(\frac{m_{\tilde{q}_i}^6 m_{\tilde{e}_{Ri}}}{m_{\tilde{u}_{Ri}}^7}\right). \quad (13)$$

We ignore the phases of SUSY breaking parameters since they do not contribute to the running of gauge couplings. In most models, the sfermion contributions to T and Ω are negligible (i.e. $X_T \sim X_\Omega \sim 1$). In particular, these contributions vanish if the masses are degenerate within the SU(5) multiplets, $\bar{\mathbf{5}}_i = (\tilde{d}_R^c, \tilde{l})_i$, $\mathbf{10}_i = (\tilde{q}, \tilde{u}_R^c, \tilde{e}_R^c)_i$. One can explicitly check that for a degenerate spectrum, $\ln\Omega = C = 0$.

To see roles of T, Ω and C in GCU, we substitute Eq. (4) into Eq. (1) and obtain

$$\frac{2\pi}{\alpha_i(Q)} = \frac{2\pi}{\alpha_G^*} - b_i \ln\left(\frac{Q}{\Omega M_G^{\deg *}}\right) + \delta_i \ln\left(\frac{T}{M_s^*}\right) + C, \quad (14)$$

where Eq. (3) has also been used.[6] It is clear that the exact unification for the general case is obtained when the rhs becomes i-independent, that is at $T = M_s^*$ [15] and the exact unification scale is given by

$$M_G = \Omega M_G^{\deg *}. \quad (15)$$

The unified gauge coupling is related to that of the degenerate case as

$$\alpha_G^{-1} = \alpha_G^{*-1} + \frac{C}{2\pi}. \quad (16)$$

Away from the exact unification, we define a candidate unification scale M_U and a semiunified coupling α_U by

$$\alpha_1(M_U) = \alpha_2(M_U) \equiv \alpha_U. \quad (17)$$

This scale can be computed from the low energy spectrum as

$$M_U = \Omega M_G^{\deg *}(T/M_s^*)^{\frac{\delta_1 - \delta_2}{b_1 - b_2}}, \quad (18)$$

where $\frac{\delta_1 - \delta_2}{b_1 - b_2} = -\frac{25}{84} \simeq -0.3$, and at this scale the gauge couplings are given by

$$\frac{2\pi}{\alpha_i(M_U)} = \frac{2\pi}{\alpha_G^*} + \left(\delta_i - b_i \frac{\delta_1 - \delta_2}{b_1 - b_2}\right) \ln\left(\frac{T}{M_s^*}\right) + C. \quad (19)$$

Using this formula, a measure of gauge coupling unification, which we define as $\epsilon_3 \equiv (\alpha_3(M_U) - \alpha_U)/\alpha_U$, is calculated as

$$\epsilon_3 = \frac{\alpha_G^*}{2\pi} Y \ln\left(\frac{T}{M_s^*}\right) + \cdots, \quad (20)$$

where the dots represent higher order terms of $\frac{\alpha_G^*}{2\pi}$ and

$$Y \equiv \frac{b_1(\delta_2 - \delta_3) + b_2(-\delta_1 + \delta_3) + b_3(\delta_1 - \delta_2)}{b_1 - b_2} = \frac{19}{14}. \quad (21)$$

It is interesting that ϵ_3 depends only on T at the leading order [15].

---

[6]Strictly speaking, γ_i and Δ_i do not cancel out in this expression, since the unification scales and the unified couplings are different between the general and the degenerate SUSY cases. However, the differences are of higher order and can be neglected.

All numerical scans presented in this paper use a two-loop RGE code including the effect of the top Yukawa coupling, following [14]. We use $\tan\beta = 10$, but a variation of $\tan\beta$ results in negligible effects. The SUSY breaking parameters are uniformly scanned in the logarithmic scale within $[m_{\min}, 10^3 \text{ TeV}]$. We take $m_{\min} = 1.5$ TeV for M_3 and 200 GeV for M_2, μ and m_A. The sfermion masses are assumed to be universal ($\equiv m_{\tilde{f}}$) for simplicity and $m_{\min} = 1$ TeV is used. We also vary $\alpha_3(m_Z) = 0.1184(7)$, according to the 1-$\sigma$ uncertainty. At the central value of $\alpha_3(m_Z)$, numerically, $M_s^* = 2.08$ TeV, $M_G^{\deg *} = 1.27 \times 10^{16}$ GeV and $\alpha_G^{*-1} = 25.5$.

We show in Fig. 1 the result of our numerical scan. The top plot in Fig. 1 confirms the predicted relation Eq. (20) (dashed line). Hereafter, we keep the points that have precise GCU, $|\epsilon_3| < 0.1\%$, and discard them otherwise. We see that the precision GCU occurs only when the SUSY masses are arranged such that T computed by Eq. (9) is within a certain range, $[1, 4]$ TeV, centred around 2 TeV. The width of T for precision GCU is generated by two factors: a variation of M_s^* corresponding to the uncertainty on $\alpha_3(m_Z)$ and a small violation of $T = M_s^*$ caused by up to 0.1% deviation from the exact unification, $\epsilon_3 = 0$. The middle plot shows the correlation between Ω and the exact unification scale, M_G. The color of points represents a typical SUSY scale $\sqrt{M_3 M_2}$. One can see that heavy SUSY tends to have a small unification scale. For the PeV scale SUSY with $\sqrt{M_3 M_2} \sim 10^3$ TeV, M_G is reduced by a factor of 5 compared to the TeV scale one. The bottom plot confirms the predicted relation Eq. (16) (dashed line). The color-code indicates a SUSY scale, $(M_3 M_2 m_{\tilde{f}})^{\frac{1}{3}}$. We see that high scale SUSY tends to predict a smaller unified coupling, α_G, but the variation is small and only up to $\sim 10\%$ between the TeV and PeV scale SUSY mass points.

An interesting observation follows from the last two plots of Fig. 1. High scale SUSY, where the unification scale is lower, in general leads to a rapid proton decay, $p \rightarrow e^+ \pi^0$. This is because the rate $\Gamma(p \rightarrow e^+ \pi^0)$ scales as $\alpha_G/(M_G)^4$, where the X, Y boson mass is identified as the unification scale, since the precise gauge unification implies all GUT particles forming incomplete GUT multiplets (e.g. X, Y bosons and colored Higgs) have the same mass, M_G. Turning this around, the lower limit on M_G from the proton lifetime measurement (if found, bearing in mind that the variation of α_U is small) can place *upper bounds* on the masses of SUSY particles. Let us denote this lower limit by M_{PD}: $M_G > M_{PD}$. Then, eliminating M_3 from Eq. (10) by using Eqs. (9) and (18) gives us

$$M_2^{\frac{4}{5}}(\mu^4 m_A)^{\frac{1}{25}} < M_s^*\left(\frac{M_{PD}}{M_G^{\deg *}}\right)^{-\frac{2016}{475}} X_{\text{EW}}^{\frac{1}{25}}, \quad (22)$$

with

$$X_{\text{EW}} \equiv \prod_{i=1\ldots3}\left(\frac{m_{\tilde{l}_i}}{m_{\tilde{d}_{R_i}}}\right)\left(\frac{m_{\tilde{q}_i}^7}{m_{\tilde{e}_{R_i}}^3 m_{\tilde{u}_{R_i}}^4}\right), \quad (23)$$
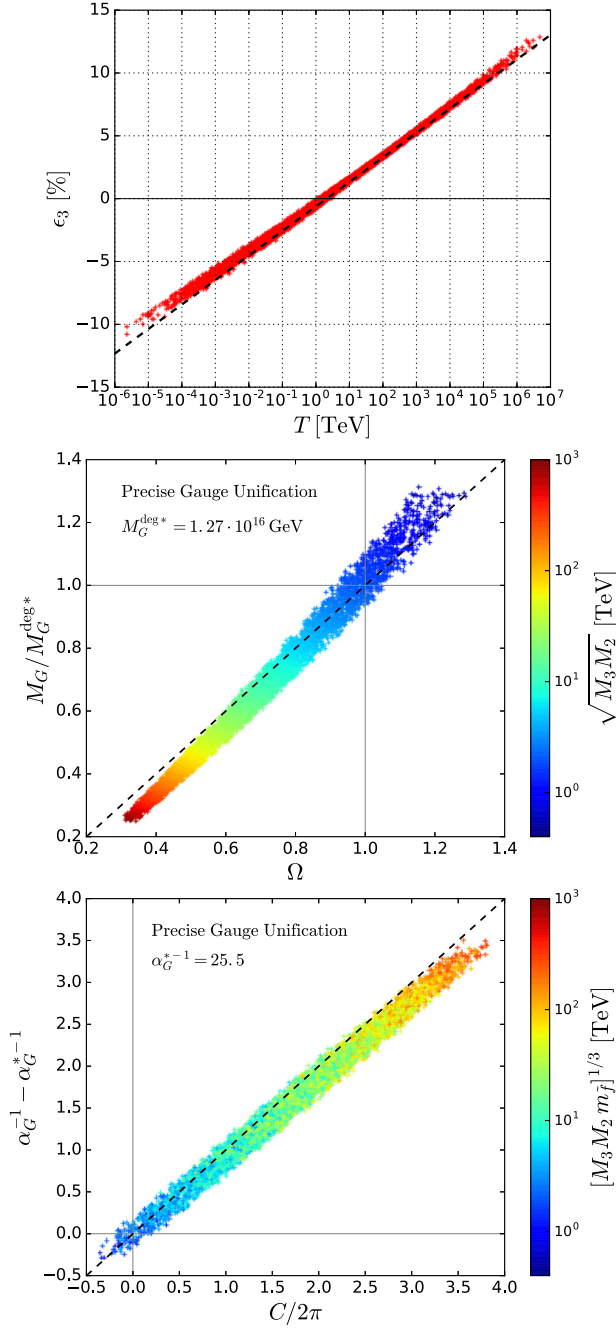
FIG. 2. Points with precise gauge unification ($|\epsilon_3| < 0.1\%$) projected onto the $\min(M_2, \mu, m_A)$ vs M_G plane. The blue, green and orange points correspond to the points where M_2, μ and m_A is the smallest among them, respectively. The regions below a black-dashed or a red-solid line are excluded by the quoted future or current limits on the proton lifetime. The black-solid line corresponds to the upper bound Eq. (22) for $T = M_s^*$ and $M_{PD} = M_G$.

FIG. 1. Scan of SUSY particle masses projected onto the (T, ϵ_3) (top), the $(\Omega, M_G/M_G^{\deg *})$ (middle) and $(C/2\pi, \alpha_G^{-1} - \alpha_G^{*-1})$ (bottom) planes. In the middle and bottom plots, the precise gauge unification ($|\epsilon_3| < 0.1\%$) is required (corresponding to the blue band in the top plot), and the color-codes represent typical SUSY scales $\sqrt{M_3 M_2}$ and $(M_3 M_2 m_{\tilde{f}})^{\frac{1}{3}}$, respectively. The dashed lines represent the two-loop relations Eqs. (20), (15) and (16) for the top, middle and bottom plots, respectively.

where $M_s^* = 2.08$ TeV and $M_G^{\deg *} = 1.27 \times 10^{16}$ GeV are the constants. This implies that the smallest mass in the lhs is bounded from above by the rhs of Eq. (22). When this bound is saturated, $M_2 = \mu = m_A$. The upper limit on the individual parameters are obtained, for example, as
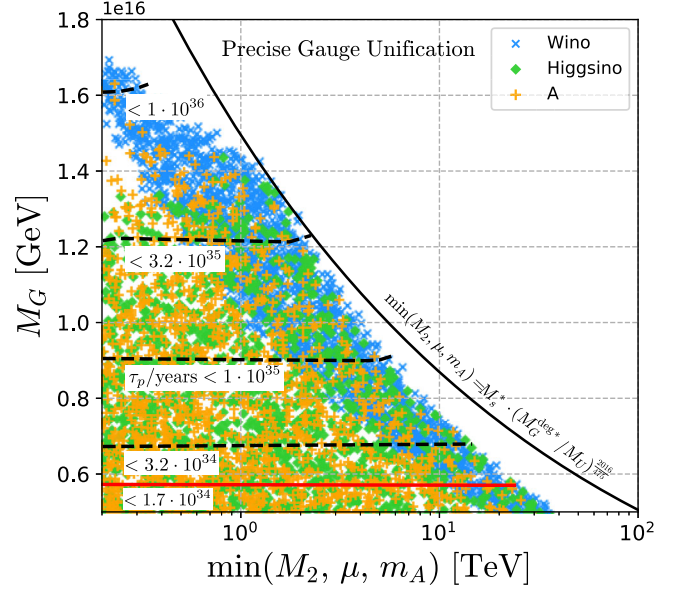
$$M_2 < M_s^* \left(\frac{\mu^4 m_A}{M_s^{*5}}\right)^{-\frac{1}{20}} \left(\frac{M_{PD}}{M_G^{\deg *}}\right)^{-\frac{504}{95}} X_{EW}^{\frac{1}{20}}, \qquad (24)$$

In this expression the rhs is bounded from above by the experimental lower limit on μ and m_A.

The upper bound Eq. (22) is observed in our numerical scan shown in Fig. 2, where the smallest of M_2, μ and m_A is plotted in the x-axis. The blue, green and orange points correspond to the cases where M_2, μ and m_A is the lightest among the three, respectively. A tendency is observed that M_2 is close to the upper limit if M_2 is the lightest. This is due to the higher power for M_2 in Eq. (22) than for μ and m_A. At each point we calculate $\tau_{p \to \pi^0 e^+}$ based on [16,17][7] using α_G and M_G obtained by the two-loop RGE code. The horizontal black-dashed and red-solid lines represent the boundaries where all points below them have the lifetime shorter than the quoted values. In particular, the region below the red line is excluded by the current limit: $\tau_{p \to \pi^0 e^+} > 1.7 \times 10^{34}$ years [19].

---

[7] The calculation of $\tau_{p \to \pi^0 e^+}$ is not completely model independent. For example, $\tau_{p \to \pi^0 e^+}$ in flipped SU(5) models is smaller by $1/[1 + (1 + V_{ud})^2] \sim 1/5$ than in conventional models [18].

The upper bound on the gluino mass can be found by eliminating $\mu^4 m_A$ in Eq. (10) by using Eq. (9) as

$$M_3 < M_s^* \left(\frac{M_2}{M_s^*}\right)^{-1} \left(\frac{M_{PD}}{M_G^{\deg *}}\right)^{-\frac{216}{19}} X_{\tilde{g}}^{\frac{1}{4}} \qquad (25)$$

with

$$X_{\tilde{g}} \equiv \prod_{i=1\ldots3} \left(\frac{m_{\tilde{u}_{Ri}} m_{\tilde{e}_{Ri}}}{m_{\tilde{q}_i}^2}\right). \qquad (26)$$

As previously, the rhs of Eq. (25) is bounded from above by the experimental lower limit on the wino mass.

If the SUSY breaking mechanism is specified, the ratio of gluino and wino masses is usually predicted. Assuming the value of $R \equiv M_3/M_2$, the following upper bounds can be derived:

$$M_3 < M_s^* R^{\frac{1}{2}} \left(\frac{M_{PD}}{M_G^{\deg *}}\right)^{-\frac{108}{19}} X_{\tilde{g}}^{\frac{1}{8}}, \qquad (27)$$

$$M_2 < M_s^* R^{-\frac{1}{2}} \left(\frac{M_{PD}}{M_G^{\deg *}}\right)^{-\frac{108}{19}} X_{\tilde{g}}^{\frac{1}{8}}, \qquad (28)$$

$$(\mu^4 m_A)^{\frac{1}{5}} < M_s^* R^2 \left(\frac{M_{PD}}{M_G^{\deg *}}\right)^{\frac{144}{90}} \cdot X_\mu^{\frac{1}{10}}, \qquad (29)$$

where

$$X_\mu \equiv \prod_{i=1\ldots3} \left(\frac{m_{\tilde{l}_i}^2}{m_{\tilde{d}_{Ri}}^2}\right) \left(\frac{m_{\tilde{q}_i}^4}{m_{\tilde{e}_{Ri}} m_{\tilde{u}_{Ri}}^3}\right). \qquad (30)$$

We show in Fig. 3 our scan in the (M_3, M_2) plane with the color-code indicating $(\mu^4 m_A)^{\frac{1}{5}}$. As previously, the black-dashed and red-solid lines represent the future and current bounds on $\tau_{p\to\pi^0 e^+}$. It is evident that M_3 and M_2 are highly sensitive to the proton lifetime and constrained by it from above. This is in direct contrast to collider searches, constraining these parameters from below. Unlike M_3 and M_2, μ and m_A are almost insensitive to the proton lifetime, which follows from the lower power of M_{PD} in Eq. (29). On the other hand, they are highly sensitive to R. In particular, μ is typically a TeV for $R \sim 1$ whereas it is $\mathcal{O}(100)$ TeV for $R \sim 7$. The implication of this to naturalness and phenomenology are studied in detail in [3,4].

It is remarkable that the current proton lifetime limit already excludes the gluino and wino masses *larger* than 70 and 70 TeV for $R \sim 1$ (compressed SUSY), 120 and 40 TeV for $R \sim 3$ (e.g. CMSSM, GMSB) and 200 and 30 TeV for $R \sim 7$ (e.g. AMSB), respectively. Next generation nucleon decay experiments are expected to improve the current
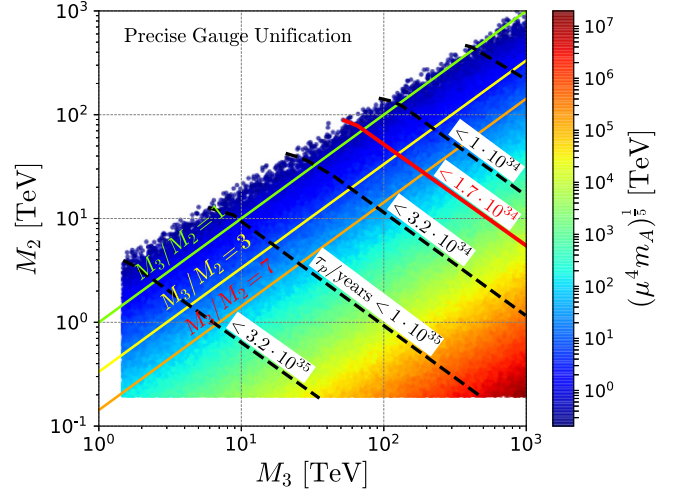

FIG. 3. Points with precise gauge unification ($|\epsilon_3| < 1\%$) projected onto the (M_3, M_2) plane. The color-code shows $(\mu^4 m_A)^{\frac{1}{5}}$. The regions above the black-dashed and red-solid lines are excluded by the quoted future or current limits on $\tau_{p\to\pi^0 e^+}$. The three diagonal lines correspond to $R \equiv M_3/M_2 = 1, 3$ and 7 from top to bottom. In this plot the upper boundaries of μ and m_A scans are extended up to 5×10^7 TeV.

$\tau_{p\to\pi^0 e^+}$ limit by a factor of ten [16], which will result in tightening the upper bounds on gluino and wino masses further down to $(M_3, M_2) \lesssim (5, 5)$ TeV for $R \sim 1$, $(10,3)$ TeV for $R \sim 3$ and $(M_3, M_2) \lesssim (15, 2)$ TeV for $R \sim 7$. These bounds are close to the lower mass limits $(M_3, M_2) \gtrsim (10, 2.7)$ TeV [20,21], which are expected to be obtained at future 100 TeV hadron-hadron colliders.

We have checked how these upper bounds are weakened if we relax the condition on the precision GUT to $|\epsilon_3| < 1\%$. In such a case, we found the current upper bounds on the gluino and wino masses to be 90 and 90 TeV for $R \sim 1$, 180 and 60 TeV for $R \sim 3$ and 280 and 40 TeV for $R \sim 7$, respectively.

It is worth noting that the above conclusion is robust against the details of the rest of the SUSY spectrum as long as sfermion masses are not split significantly within the SU(5) multiplets. In fact, the impact of nondegenerate sfermion masses on the superpartner mass bounds can be understood by, for instance, Eqs. (26) and (27). Typically, the squark and slepton masses split due to the RGEs and become $m_{\tilde{u}_{R_i}} \sim m_{\tilde{q}_i} \sim 3 m_{\tilde{e}_{R_i}}$ at the TeV scale. In this case, the gluino mass bound is even tightened by a factor of 0.7 for a fixed R. Our conclusion also holds even if new particles, which are singlets under the SM gauge group, are added to the MSSM, as in the case of the next-to-minimal supersymmetric Standard Model.

We have investigated the link between the proton lifetime $\tau_{p\to\pi^0 e^+}$ and the supersymmetric spectrum under the assumption of small GUT thresholds. It has been shown that most of the allowed mass range of gluinos and winos will be probed by future collider and proton lifetime

experiments. It is straightforward to extend this analysis to concrete models with sizeable threshold corrections. In this case, the result will depend on the details of the GUT models (see e.g. [22]).

[1] For early references see, P. Langacker, Phys. Rep. **72**, 185 (1981).

[2] N. V. Krasnikov, JETP Lett. **61**, 245 (1995); Phys. Lett. B **392**, 365 (1997); arXiv:hep-ph/9710520.

[3] S. Raby, M. Ratz, and K. Schmidt-Hoberg, Phys. Lett. B **687**, 342 (2010).

[4] S. Krippendorf, H. P. Nilles, M. Ratz, and M. W. Winkler, Phys. Rev. D **88**, 035022 (2013); H. P. Nilles, Adv. High Energy Phys. **2015**, 1 (2015).

[5] S. Raby, *Supersymmetric Grand Unified Theories* (Springer International Publishing, Gewerbestrasse, 2017).

[6] A. Hebecker, J. High Energy Phys. 01 (2004) 047; A. Hebecker and M. Trapletti, Nucl. Phys. **B713**, 173 (2005); A. Anandakrishnan and S. Raby, Nucl. Phys. **B868**, 627 (2013).

[7] K. R. Dienes, E. Dudas, and T. Gherghetta, Nucl. Phys. **B537**, 47 (1999); Phys. Lett. B **436**, 55 (1998); Y. Kawamura, Prog. Theor. Phys. **105**, 999 (2001); L. J. Hall and Y. Nomura, Phys. Rev. D **64**, 055003 (2001); A. Hebecker and M. Trapletti, Nucl. Phys. **B713**, 173 (2005).

[8] S. A. R. Ellis and J. D. Wells, Phys. Rev. D **91**, 075016 (2015); **96**, 055024 (2017).

[9] G. F. Giudice and A. Strumia, Nucl. Phys. **B858**, 63 (2012); M. Ibe and T. T. Yanagida, Phys. Lett. B **709**, 374 (2012); E. Bagnaschi, G. F. Giudice, P. Slavich, and A. Strumia, J. High Energy Phys. 09 (**2014**) 092.

[10] N. Arkani-Hamed, A. Delgado, and G. F. Giudice, Nucl. Phys. **B741**, 108 (2006); J. Hisano, S. Matsumoto, M. Nagai, O. Saito, and M. Senami, Phys. Lett. B **646**, 34 (2007); J. Ellis, F. Luo, and K. A. Olive, J. High Energy Phys. 09 (2015) 127.

[11] J. Hisano, H. Murayama, and T. Yanagida, Nucl. Phys. **B402**, 46 (1993); Phys. Rev. Lett. **69**, 1014 (1992).

[12] H. Georgi, Phys. Lett. **108B**, 283 (1982); B. Grinstein, Nucl. Phys. **B206**, 387 (1982); A. Masiero, D. V. Nanopoulos, K. Tamvakis, and T. Yanagida, Phys. Lett. **115B**, 380 (1982); K. S. Babu, I. Gogoladze, and Z. Tavartkiladze, Phys. Lett. B **650**, 49 (2007).

[13] L. J. Hall, Nucl. Phys. **B178**, 75 (1981); M. B. Einhorn and D. R. T. Jones, Nucl. Phys. **B196**, 475 (1982); U. Amaldi, W. de Boer, and H. Furstenau, Phys. Lett. B **260**, 447 (1991).

[14] P. Langacker and N. Polonsky, Phys. Rev. D **47**, 4028 (1993).

[15] M. Carena, S. Pokorski, and C. E. M. Wagner, Nucl. Phys. **B406**, 59 (1993).

[16] K. S. Babu *et al.*, arXiv:1311.5285.

[17] B. Bajc, J. Hisano, T. Kuwahara, and Y. Omura, Nucl. Phys. **B910**, 1 (2016).

[18] H. Murayama and A. Pierce, Phys. Rev. D **65**, 055009 (2002).

[19] V. Takhistov (Super-Kamiokande Collaboration), arXiv:1605.03235.

[20] T. Cohen, T. Golling, M. Hance, A. Henrichs, K. Howe, J. Loyal, S. Padhi, and J. G. Wacker, J. High Energy Phys. 04 (2014) 117.

[21] M. Low and L. T. Wang, J. High Energy Phys. 08 (2014) 161.

[22] J. Hisano, T. Kuwahara, and N. Nagata, Phys. Lett. B **723**, 324 (2013); A. Hebecker and J. Unwin, J. High Energy Phys. 09 (2014) 125.